Paving the way for suitable metasurfaces' measurements under oblique incidence: Mono/Bi-static and Near/Far Field concerns

Humberto Fernández Álvarez, María Elena de Cos Gómez and Fernando Las-Heras

***Abstract*— This paper aims at contributing to the specialized literature on experimental characterization of metasurfaces reflectivity. Growing demand on angularly stable metasurfaces reinforces the relevance of the results under oblique incidence.**

Generally, reflection coefficient phase measurements are more challenging than the amplitude ones. Thus, an artificial magnetic conductor (AMC) is used to analyze the critical aspects for enlarging the angular margin that can be properly measured. The importance of the retrieving methodology along with the proposed data post-processing is highlighted among the involved issues, according to the obtained results.

The suitability of monostatic vs bi-static measurement set-ups for comparison with plane-wave simulation is studied. The aforementioned AMC is experimentally characterized using both set-ups providing relevant conclusions.

The trade-off between the manufactured prototype dimensions (to resemble the simulated infinite one) vs the required anechoic chamber size (to fulfil far-field (FF) conditions i.e. plane wave incidence for the considered frequencies) is tackled. Indeed, a thorough literature revision shows that most authors do not have this key aspect into account. The relevance of the resulting error from comparisons between near-field (NF) retrieved measurements vs plane-wave simulation results is unveiled. This is even more critical when the angular stability is analysed, since the scattering patterns of the AMC are not conformed at near-field distances, which makes the errors even greater. Consequently, noteworthy conclusions concerning the characterization of AMCs in particular and metasurfaces in general, regarding far-field or near-field measurements and angular stability analysis will be presented.

***Index Terms*— Metamaterial; metasurface; Far-Field measurement; Near-Field measurements; angular stability; artificial magnetic conductor; reflectivity.**

I. INTRODUCTION

Metasurfaces (MTSs) have been attracting much attention during the recent years, due to their amazing capabilities of interaction with electromagnetic waves. Indeed, they have been used in many applications aiming at, for example, improving the radiation properties of antennas, modifying the reflectivity of objects (above all in Radar Cross Section (RCS) variation) or reducing the Specific Absorption Rate (SAR), among others. A thorough review of the literature contributions unveils a severe problem concerning the experimental characterization of metasurfaces: a vast majority of works present measurements conducted under near-field conditions, even when the authors stated that they were performed under far-field ones. The latter is attributed to the fact that the metasurface dimensions were not taken into consideration. Therefore, the comparison between simulations (conducted under far-field conditions) and measurements (conducted under near-field ones) are not valid at all even when they look alike. This is especially critical when characterizing the angular stability of metasurfaces and their reflection coefficient phase. Consequently, artificial magnetic conductors (AMCs) seem to be an ideal metasurface to study the aforementioned problems in characterizing the reflectivity, since the reflection coefficient phase has to be measured.

AMCs are categorized as metasurfaces, exhibiting a phase variation with frequency from -180º to 180º and crossing 0º at their resonance [1]-[4]. They are employed in many applications, mostly combined with antennas to improve their radiation properties (gain, efficiency etc.) [5]-[6]. However, they are also used to modify the propagation of the incident electromagnetic waves. Consequently, they can change the polarization of the wave [7] or when combined with a Perfect Electric Conductor (PEC) or other AMC, they can control the scattering from the whole structure and reduce the RCS.

Many papers have been devoted to improve the AMC properties, such as its bandwidth [9] or to achieve multiresonance [10]. However, as it was previously mentioned, its experimental verification, as it occurs with other metasurfaces, has not always been conducted properly [11], above all when the angular stability of the metasurface is under study [1],[12]-[13]. As it was mentioned, a great amount of literature contributions do not conduct the experimental validation under far-field conditions, even when it is said that they are performed under this condition. The latter is attributed to the fact that the authors do not consider the electrical size of the manufactured prototype, which should be taken into account when conducting scattering measurements [14], since the impinging wave on the metasurface is coupled and reradiated. Therefore, they do not apply the pertinent near-field to far-field transformation [15], which is not always trivial [16], especially when the metasurface is excited under different incidence angles [17].

An alternative for evaluating large planar structures at distances smaller than the required by the far-field condition is adopted in [18]. In this article, a scanning free-space system is employed to measure the absorption of a microwave absorber. During this measurements highly directive transmitting and receiving antennas are used, which allows the structure to be locally illuminated by a plane wave. However, this method just gives an idea of the absorber's absorption. On the other hand, the use of lenses can also be an alternative [19]-[20]. These lenses focus most of the energy on the structure, ensuring that a plane wave impinges on it. Moreover, they can also be employed to reduce diffraction from the structure's edges [18]. Nevertheless, these lenses have to be designed and manufactured ad hoc for each application and they can introduce certain uncertainties in the measurements.

In [21], a technique for measuring the absorption of electromagnetic waves by a metamaterial is presented. However, for measuring the absorption only the amplitude of the scattering field is considered, being the phase a parameter that requires a more precise set-up arrangement [22]. Moreover, most of the problems that arise when characterizing a metasurface (or a planar structure) under different incidence angles and antenna arrangements are not considered. Indeed, the latter is crucial for determining whether the metasurface behaves as desired or not.

In this paper, the considerable errors of characterizing the angular stability of metasurfaces in an anechoic chamber, when the far-field condition is not fulfilled, will be analysed and compared with the simulation results (which are conducted under this condition). The latter errors are specially critical when measuring the reflection coefficient phase of a metasurface. Moreover, the optimum configuration of the measurement set-up is of utmost importance in the measurement of the metasurfaces' angular stability. Consequently, considering the AMC introduced in a previous work [23], a significant advances in the state of art, regarding the presented in [11]-[15],[18]-[21],[23], will be introduced in this paper, devoting special attention to the influence of the angular step at which the measurements are retrieved, as well as the necessity of conducting a suitable statistical treatment of the measured data. Therefore, the same prototype as in [23] will be considered and measured under both a quasi-monostatic (as in the cited paper) and bistatic set-up configurations. In the quasi-monostatic set-up, the transmitting and receiving antennas are kept fixed, while the prototype is rotated. However, in the bistatic set-up the prototype is kept fixed and the antennas are shifted along low-reflecting benches, so that the measurements are taken at specular angles. From the study of both set-ups, several recommendations will be extracted. Moreover, the measurement results will unveil great differences on the resulting measurable angular margin, provided such recommendations are considered or not.

II. Materials and Methods

The first step prior to conducting the measurements in an anechoic chamber is to confront the required distance to measure under far-field conditions (taking into consideration the metasurface and antennas dimensions and the highest frequency of interest) with the anechoic chamber dimensions. Either the metasurface dimensions should be shortened and/or different antennas have to be used if the far-field conditions were not fulfilled.

The AMC presented in [23], which exhibits improved angular stability, will be also experimentally analysed in this paper. Its unit-cell, which is depicted in Fig.1(a), comprises a hexagonal loop metallization on a grounded RO4003C dielectric ($\varepsilon_r = 3.38$ and $tan\delta = 0.0027$) with thickness 1.524 mm. The same geometric parameters as in [23] will be considered in this paper: $p = 11.25\,mm$, $w = 5.46\,mm$, $g = 0.9\,mm$, and $l = 1.6\,mm$. Additionally, the manufactured prototype will comprise an identical number of unit-cells as in [23] (29x19 unit-cells), so that its total size is $283x214x1.524\ mm^3$ (see Fig.1(b)). Therefore, fairly comparisons with the measurement results presented in [23] can be conducted. The distance to meet the far-field conditions [24], considering the dimensions of the AMC and the measurement antennas (Narda 642 waveguide horn antennas, whose aperture size is 118.62x89.66 mm^2), as well as the range of frequencies that are wanted to be measured (5.5GHz to 6.6 GHz), is 5.39 m $\left(\frac{2D^2}{\lambda}\right.$, being $D = \sqrt{28.3^2 + 21.4^2}\ cm \approx 0.35\ m$ and $\left.\lambda = \frac{3\ 10^8}{6.6\ 10^9}\right)$. The measurements will be conducted in an anechoic chamber, whose maximum measurable distance (5.35 m) is roughly the same as the one needed to meet the previous requirement. Both quasi-monostatic and bistatic measurements will be retrieved by properly arranging the transmitting and receiving antennas, as it was mentioned in the previous section.

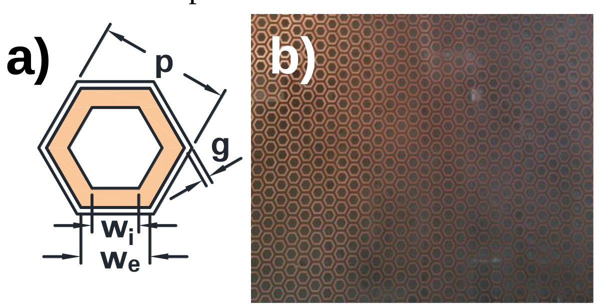

Fig.1. Unit-cell of the AMC (a). Manufactured prototype (b).

On the other hand, the AMC will be measured at a shorter distance inside the Fresnel region (1.3 m) and compared with the measurements conducted at far-field, aiming to show the differences on the retrieved measurements at both distances. This study is presented to reflect the necessity of characterizing metasurfaces under far-field conditions, above all when different incidence angles are wanted to be measured (due to the significant error introduced in the measurements if the mentioned condition is not satisfied) and the derived consequences that arise (proper operation of the metasurface or not). It should be noticed that the vast majority of contributions in the literature do not conduct the measurements under a far-field condition over the whole range of analysed frequencies, since they do not take into account the finite metasurface dimensions.

III. Results and Discussion

As it was pointed out in the introduction, one of the major problems in experimentally characterizing the reflection coefficient of a metasurface (and hence, its angular stability) resides in conducting the measurements under near-field conditions and comparing them with what it is simulated (under far-field conditions). A comparison between measurements on which this condition is satisfied or not will be presented in C, as well as the main undesired consequences. However, firstly it is wanted to clarify how to properly optimize the measurement set-up, even when the authors properly conduct the measurements under far-field conditions. The latter will be tackled by considering both monostatic and bistatic set-up configurations.

A. Quasi-monostatic measurements

Even when the metasurfaces' measurements are conducted under far-field conditions, most of the literature contribution do not take into account crucial considerations to make the most of the measurement set-up. This is even more noticeable when the metasurface's angular stability is wanted to be characterized in an anechoic chamber. Indeed, as the authors know that there will be certain limitations on the range of angles that can be measured, they will resign to measure just a few ones [23].

Consequently, in this section some new considerations will be introduced and the ones previously presented in [11] will be also contemplated, aiming at optimizing the set-up for making the most of it. Then, the measurements will be compared with the ones previously presented in [23], which although they are properly conducted, the recommendations introduced in this paper have not been considered. The latter will show the importance of properly arranging the set-up and conducting the data post-processing proposed here. Apart from the recommendations introduced in [11], it is crucial to consider the following ones:

- A novel and larger absorptive structure (see Fig.2(a)) is used to minimize edge diffraction.
- The antennas are oriented facing the prototype using a laser level and the positioner system, which has an angular resolution of 0.1º, is moved in steps of 0.5º instead of 2º (as in [23]). The latter will be useful to properly correct slight misalignments on the position of both the AMC and the calibration prototype (metallic plate).
- Measurements are conducted with an empty chamber (no prototype on the pylon) [18], after and before the AMC or the metallic plate is placed on the pylon. This will help to ensure that no undesired echo or instrumentation error are introduced in the set-up between measurements.
- Several measurements are taken for each incidence angle for both the AMC and the metallic plate, in order to ensure their repeatability. The latter also allows reducing the receiver noise by applying proper data processing (statistical functions). In addition, a temporal windowing (time gating) is used to record just the desired echo from the measured prototype (AMC or metallic plate).

From these four points, it may result obvious that the antennas have to be oriented facing the prototype and it is not new that the measurement of the empty chamber can alert about the existence or not of unwanted echoes. Moreover, some previous works surround the metasurface with absorbers to avoid edge diffraction. However, there are two key points that provide new knowledge, being the most critic one the necessity of measuring the metasurface at small angular steps of the incident wave. Indeed, the majority of works just take into account the incident angles considered in simulation (in 10º, 15º or 20º degree step). In fact, in our previous work [23] a step of 2º is chosen for measuring the metasurface and no misalignement correction were conducted on the retrieved measurements. Therefore, measuring the metasurface using a finer angular step will allow us to correct the mentioned misalignements, which is not considered in other literature contributions (including the author's one [23]) and it is a crucial aspect for enlarging the angular margin that can be properly measured. Moreover, although it is known that a statistical treatment of the measured data reduces the measurement uncertainties, the one that will be introduced in this paper, does not only contribute to reinforce the previous idea, but also reveals that as phase measurements are taken, this aspect is specially critic.

The anechoic chamber set-up configuration is schematically depicted in Fig.2(a) and Fig.2(b) for both TE and TM polarizations. This set-up arrangement is similar to the one presented in [11] for the configurations on which best measurement results are obtained in that paper. The parameter α in Fig.2(b) is the angle between the transmitting and receiving antennas line of sight on the metasurface. In this case, the recommendations described above are applied and the positioner system, on which the AMC or metallic plate will be placed, is located at the maximum measurable distance of the chamber (at the beginning of the slider (see pictures)) to meet far-field conditions. The distance between the transmitting and receiving antennas will be fixed to be $d_{ant} = 25\ cm$ for the TE polarization and $27\ cm$ for the TM one (similar to the one considered in [23]). As in [11], the scattering pattern of both the AMC and the metallic plate are retrieved, aiming to adjust slight misalignments between the position of both and also determine the angular margin that can be measured, in accordance with the available dynamic range for each incidence angle. The latter is properly explained in the mentioned paper and will not be repeated here.

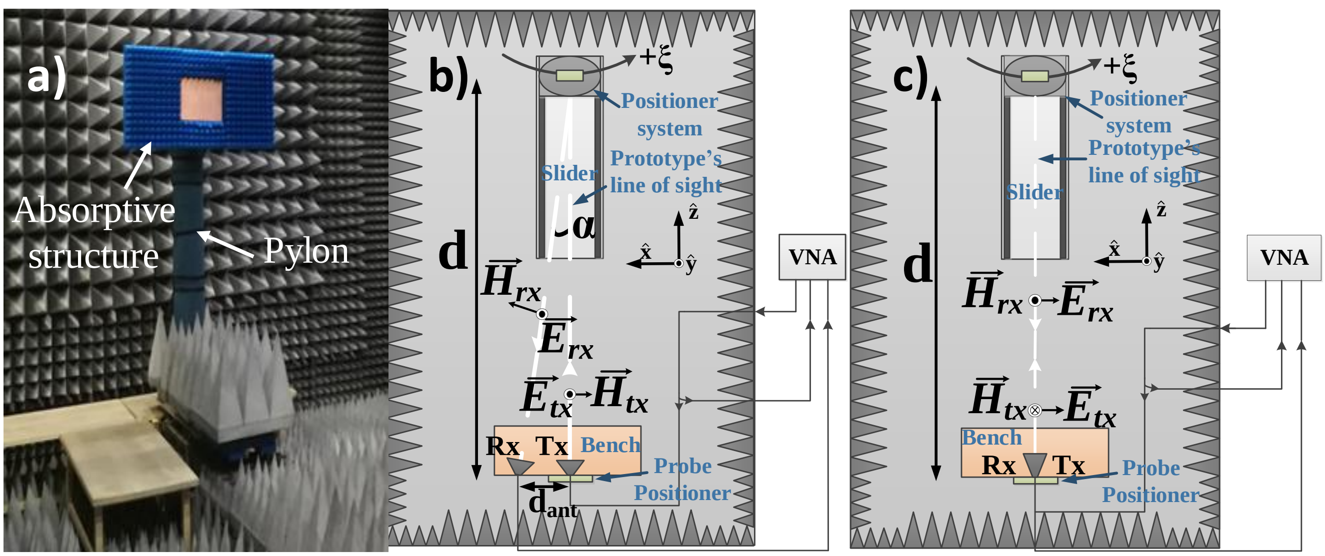

Fig.2. AMC on the positioner with the surrounding absorptive structure (a). Quasi-monostatic set-up configuration under TE (b) and TM (c) polarizations.

The phase measurement results after applying the previous mentioned post-processing procedures, consisting of adjusting the positioning misalignments, subtracting the acquired phase of the AMC from the one of the metallic plate as explained in [23] and reducing the retrieved noise (using statistical functions), are presented in Fig.3 and Fig.4 for TE and TM polarizations, respectively. The incident angle will be denoted as "θ" throughout the article.

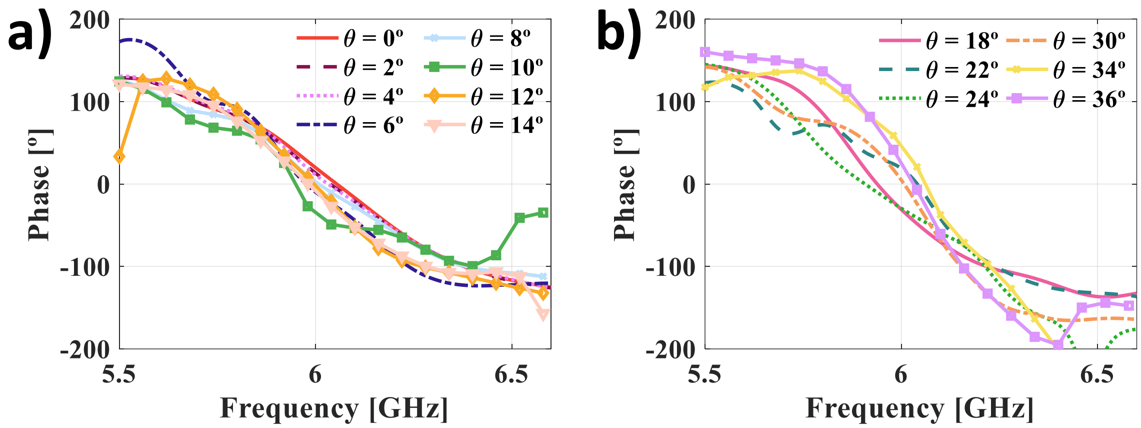

Fig.3. Quasi-monostatic measurements for TE polarization under different incidence angles: from 0º to 14º (a) and from 18º to 36º (b).

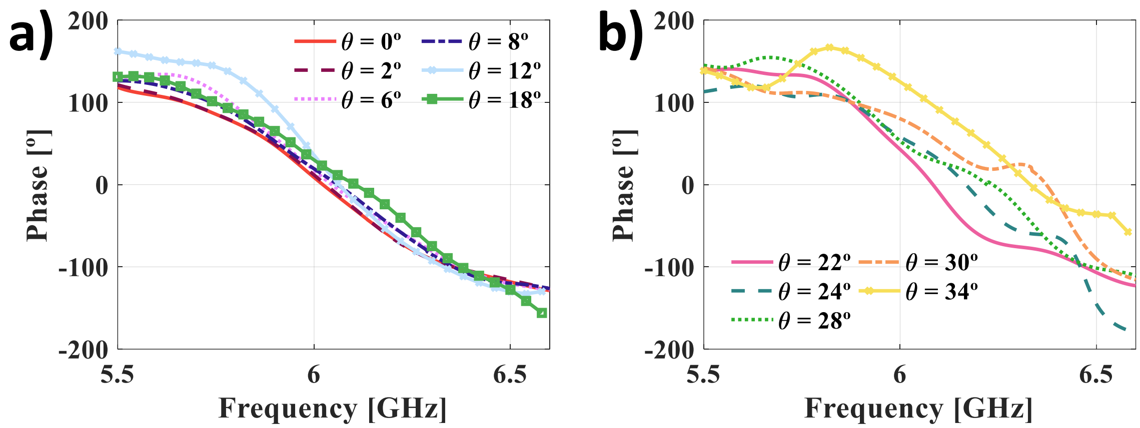

Fig.4. Quasi-monostatic measurements for TM polarization under different incidence angles: from 0º to 18º (a) and from 22º to 34º (b).

The angular margin that can be properly measured is from 0º to 36º and from 0º to 34º for TE and TM polarizations, respectively. It should be mentioned that there are some angles within these ranges that cannot be properly measured, due to the lack of a suitable dynamic range as it was mentioned in [11] and [23]. However, following the previous recommendations, it can be noticed that the angular range measured here almost double the one reached in [23] (0º to 18º). The latter is attained by carefully following the previously presented considerations.

B. Bistatic measurements

Another alternative to experimentally characterize the AMC under different incidence angles is by resorting to a bistatic configuration set-up. Pictures of the antennas arrangement on the anechoic chamber and a scheme of the set-up configuration for both TE and TM polarizations are presented in Fig.5. As it can be noticed, the positioner is once more placed at the maximum measurable distance of the anechoic chamber to ensure that the measured data are retrieved under far-field conditions.

The measurements are presented in Fig.6. The inferior limit for the angular margin is determined by the minimum distance between antennas that ensures no coupling between them. The superior limit is restricted by several factors: the anechoic chamber width, the AMC dimensions and the required frequency range (which determine the far-field distance) and the capability to properly couple the incident field on the AMC at large incidence angles. It should be noticed that a bistatic set-up allows measuring a smaller angular margin for the analysed metasurface than a quasi-monostatic one. The latter is due to the large prototype size, which implies meeting far-field condition at long distances and thus, requires large separation between the antennas to impinge on the prototype at high oblique incidence angles. In this case, as the maximum separation between antennas that ensures a proper coupling of the incident wave on the prototype is 2 m, the maximum angle that can be measured is 10º $\left(\tan^{-1}\left(\frac{1\,m}{5.35\,m}\right) \approx 10^{\circ}\right)$. This angular margin can be increased by reducing the prototype size, but the latter should be enough large to exhibit a similar performance than its infinite counterpart.

Under this set-up configuration, there is no intermediate angle that cannot be measured, as it occurs when a quasi-monostatic configuration is considered, since the measurements are taken at the specular direction. Therefore, there is no lowering on the dynamic range under certain incidence angles, as long as the incident wave is properly coupled on the AMC.

It should be noticed that the distinction between a monostatic and a bistatic configuration is not needed to be done in simulations, when the metasurface is considered infinite. Indeed, both configurations can be considered as being identical. However, in practice the metasurface will be finite and hence, these two measurements have to be taken into account. As long as the metasurface is isotropic, it should be noticed that the bistatic ones may be more suitable for comparing with the simulations (which was not clearly specified in the state of the art). The reason is that these measurements are taken at specular angles. Nevertheless, one can notice that the monostatic characterization of a metasurface is also of crucial importance, due to the existence of many monostatic radar systems (AMCs can be used as checkerboard to redirect the scattered waves and hence, reduce the RCS).

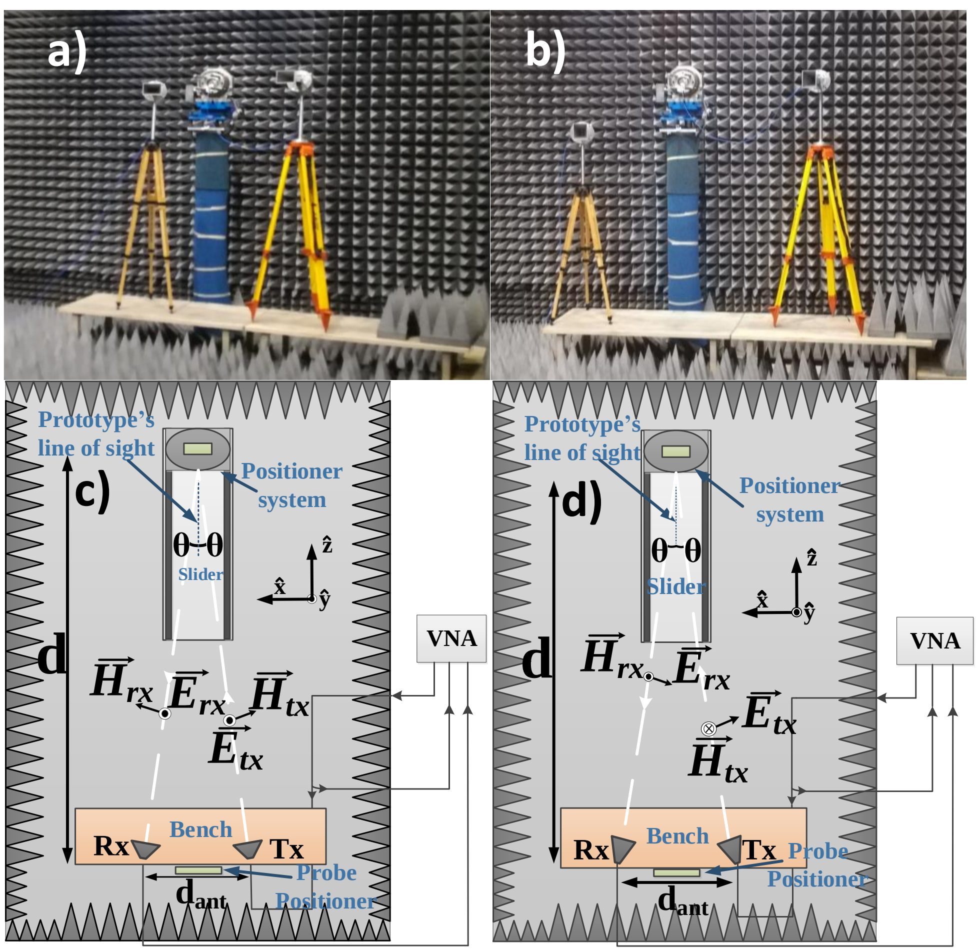

Fig.5. Pictures of the antennas arrangement on the anechoic chamber for TE (a) and TM (b) polarizations. Bistatic set-up configuration under TE (c) and TM (d) polarizations.

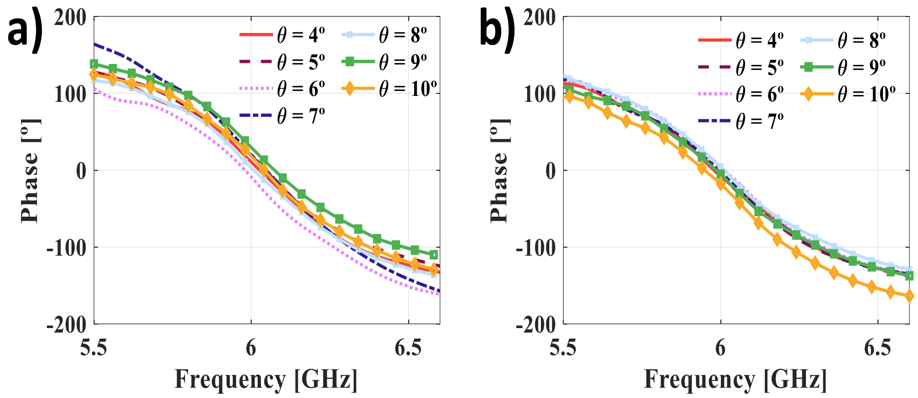

Fig.6. Bistatic measurements for TE (a) and TM (b) polarizations under different incidence angles.

C. *Far-Field versus Near-Field measurements.*

Once the previous measurements have been introduced under the far-field condition, the set-up is arranged to measure the prototype at a shorter distance inside the Fresnel region (1.3 m). For doing so, the low-reflecting benches are approached to the slider and the positioner is placed at the minimum measurable distance of the chamber. The measurements will be conducted using a quasi-monostatic set-up configuration. The distance between the transmitting and receiving antennas is identical to the one mentioned in the previously presented quasi-monostatic measurements (25 cm and 27 cm for TE and TM polarization, respectively). The measured results, after applying identical post-processing techniques as mentioned above, are presented in Fig.7.

From these results, it can be seen that the phase does not varies between -180º and 180º, which would be the expected result from the AMC behaviour. In addition, the resonance is shifted downwards (as compared to the results obtained in Fig.3 and Fig.4). The latter observations can be attributed to the near-field effects. In fact, if one considers the scattering pattern of the AMC at its resonance frequency under a far-field distance (5.35 m) and the one obtained in this section at 1.3 m, different results are clearly obtained. These patterns are shown in Fig.8. It can be noticed that the patterns at a near-field distance are not conformed. Indeed, the secondary lobes have not been formed yet.

At this point, it is possible to be mentioned that many authors consider the far field distance as $\frac{2D^2}{\lambda}$, being "D" the maximum dimension of the antenna [25]. Under this supposition and considering the measurement antennas previously cited (whose aperture dimensions are 118.62x89.66 mm^2) the supposed far-field distance is 0.97 m. This distance is shorter than the one considered in this section (1.3 m). However, as one can see inaccurate measurements are obtained when choosing this criterion, due to the near-field contamination.

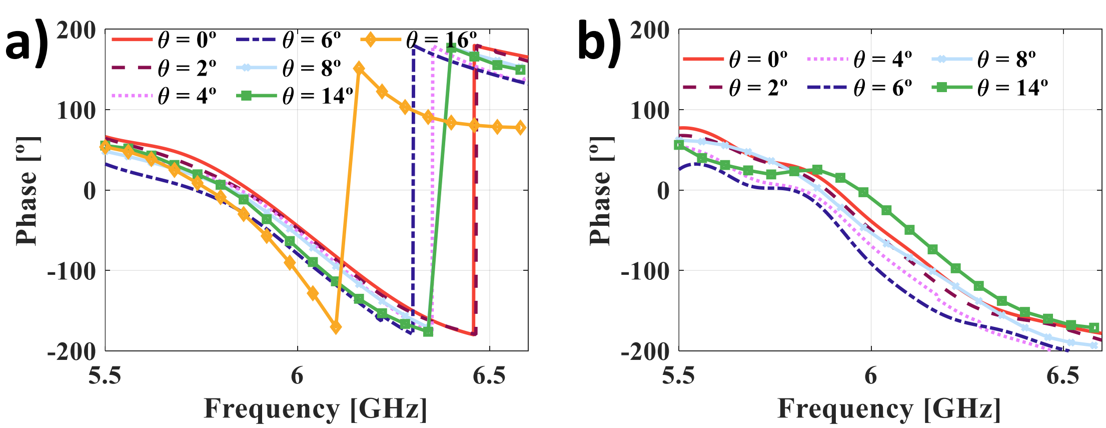

Fig.7. Quasi-monostatic measurements under different incidence angles: for TE polarization (a) and for TM polarization (b) at 1.3 m (near-field region).

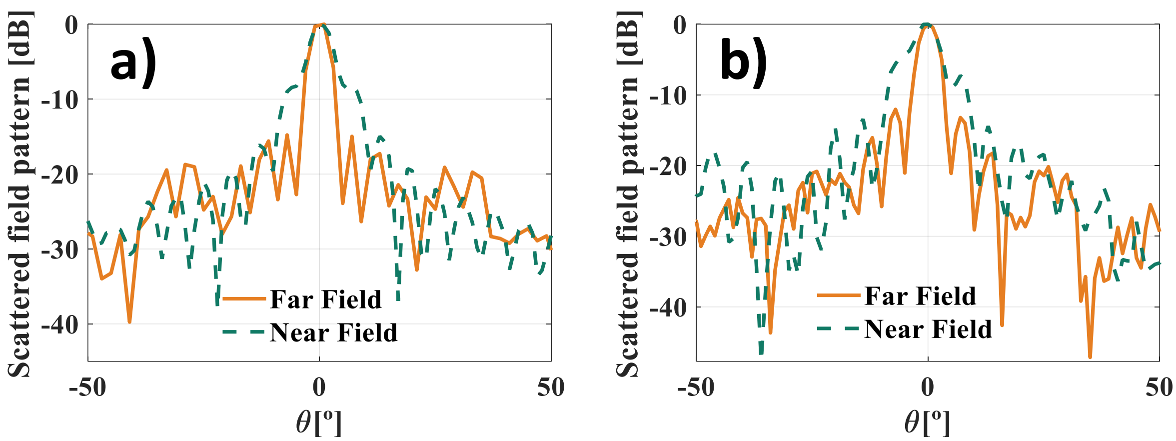

Fig.8. Quasi-monostatic measurement of the AMC scattering pattern for TE (a) and TM (b) at far-field and near-field distances.

On the other hand, the non-conformed secondary lobes may provide a higher dynamic range to measure a large angular margin when characterizing metasurfaces. However, the measurements are inaccurate, since as the scattering pattern is not conformed, when the metasurface is moved further away from the antenna this pattern will change and hence, the retrieved measurement results (phase, absorption etc.). Indeed, it is just at the far-field distance where the scattering pattern does not vary and therefore, identical measurements can be extracted even when the metasurface is moved further away. The latter is subject to the availability of suitable dynamic range in the set-up. On this matter, it should be pointed out that conducting the measurements at near-field distances can give rise to an erroneous classification of the metasurface, considering it as if it properly works when it does not or vice versa.

D. General conclusion for metasurface measurements

From the authors experience some additional and general conclusions can be drawn, regarding the experimental verification of metasurfaces. Suitable absorption results are obtained when measuring metasurface absorbers (in which just amplitude information is needed) under normal incidence, even when these measurements are retrieved on the Fresnel region, since the main lobe of the scattering pattern at 0º does not greatly vary as compared to the one obtained at far-field. However, the characterization of metasurface absorbers under different incidence angles using a quasi-monostatic set-up configuration, is not valid when conducted at near-field distances in the sense of being comparable with their performance at far-field. Indeed, as it was mentioned the scattering pattern and above all its secondary lobes are not conformed and different measurement results will be obtained at different distances in this region. In the case of considering a bistatic configuration, as the measurements are retrieved in the specular direction (maximum of the scattering pattern (0º), which does not vary sharply between the near- and far-field region), the latter is not so critic and the measurements could be considered sufficiently valid. However, it should be recognized that the measurements are taken in the near-field region, which introduce slight inaccuracies on the results.

It should be noticed that measuring the phase response of metasurfaces is a more arduous problem than measuring their amplitude. Indeed, the phase is the widely employed parameter which determines a suitable measurement error and it is used to define the far-field condition. Consequently, when measuring the phase of a metasurface in the near-field region larger errors will be introduced in the measurements than if its amplitude were measured, under either a quasi-monostatic or bistatic configuration.

IV. Conclusions

In this paper, the severe problems that entail not measuring a metasurface under far-field conditions, especially when its angular stability is wanted to be characterized are shown. For illustrating that, measurements at near-field and far-field distances of an AMC's reflection coefficient phase were retrieved and the magnitude of the committed error was illustrated, giving special attention to the characterization of the metasurface's angular stability. Indeed, the latter can give rise to categorize a metasurface as being operative when it is not. Moreover, important considerations regarding the measured data post-processing have been presented, making special emphasis in the correction of misalignments between the metasurface and the calibration prototype and the statistical treatment of the measured data. It has been shown that the latter can lead to double the measurable angular margin obtained in [23], when considering a quasi-monostatic set-up. Moreover, the metasurface is also characterized under a bistatic set-up configuration and the restrictions of both set-ups when arranged on an anechoic chamber have been introduced, as well as which could be more suitable for comparing with the infinite simulations. Furthermore, the importance of choosing suitable prototype dimensions has been highlighted.

In addition, several general recommendations regarding the experimental validation of metasurfaces behaviour, not only at normal incidence but also at an oblique one, are provided. The latter can be useful for authors to properly characterize their prototypes for their final intended application, knowing the limitations that may encounter in their laboratories.

In a future contribution, the problem on the measurable angular margin of metasurfaces can be tackled from an analytical and simulation point of view, aiming at comparing the obtained results with the measurement ones presented in this paper. Taking into account that on one hand the analytical calculations will provide a rough approximation to the problem and on the other hand, the feasible model of the measurement set-up may result unattainable (lack of data to properly reproduce the set-up elements and large computational burden), the problem could be addressed in a future contribution starting, for example, from a simplified model.

Acknowledgement

This research was partially funded by the Government of the Principality of Asturias (PCTI) and European Union (FEDER) under grant IDI/2018/000191 and under the Severo Ochoa grant BP16024.

References

[1] A. Monorchio, G. Manara and L. Lanuzza, "Synthesis of artificial magnetic conductors by using multilayered frequency selective surfaces," in IEEE Antennas and Wireless Propagation Letters, vol. 1, pp. 196-199, 2002.

[2] F. Capolino, "Theory and phenomena of metamaterials," CRC press.

[3] M. E. de Cos, F. L. Heras and M. Franco, "Design of Planar Artificial Magnetic Conductor Ground Plane Using Frequency-Selective Surfaces for Frequencies Below 1 GHz," in IEEE Antennas and Wireless Propagation Letters, vol. 8, pp. 951-954, 2009.

[4] Y. Kim, F. Yang and A.Z. Elsherbeni, "Compact artificial magnetic conductor designs using planar square spiral geometries," in Progress In Electromagnetics Research, vol. 77, pp. 43-54, 2007.

[5] F. Rahmadani and A. Munir, "Microstrip patch antenna miniaturization using artificial magnetic conductor," 2011 6th International Conference on Telecommunication Systems, Services, and Applications (TSSA), Bali, 2011, pp. 219-223.

[6] A. P. Feresidis, G. Goussetis, Shenhong Wang and J. C. Vardaxoglou, "Artificial magnetic conductor surfaces and their application to low-profile high-gain planar antennas," in IEEE Transactions on Antennas and Propagation, vol. 53, no. 1, pp. 209-215, Jan. 2005.

[7] Dunbao Yan, Qiang Gao, Chao Wang, Chang Zhu and Naichang Yuan, “A novel polarization convert surface based on artificial magnetic conductor,” 2005 Asia-Pacific Microwave Conference Proceedings, Suzhou, 2005, pp. 2.

[8] M. E. de Cos, Y. Álvarez and F. Las-Heras, “RCS reduction using a combination of artificial magnetic conductors,” Proceedings of the 5th European Conference on Antennas and Propagation (EUCAP), Rome, 2011, pp. 1336-1340.

[9] R. Diaz, “Magnetic loading of artificial magnetic conductors for bandwidth enhancement,” IEEE Antennas and Propagation Society International Symposium. Digest. Held in conjunction with: USNC/CNC/URSI North American Radio Sci. Meeting (Cat. No.03CH37450), Columbus, OH, 2003, pp. 431-434 vol.2.

[10]M. Mantash and A. Tarot, “On the bandwidth and geometry of dual-band AMC structures,” 2016 10th European Conference on Antennas and Propagation (EuCAP), Davos, 2016, pp. 1-4. doi: 10.1109/EuCAP.2016.7481589.

[11]H. Fernandez Alvarez, M. E. de Cos Gomez and F. Las-Heras, “Angular Stability of Metasurfaces: Challenges Regarding Reflectivity Measurements [Measurements Corner],” in IEEE Antennas and Propagation Magazine, vol. 58, no. 5, pp. 74-81, Oct. 2016.

[12]D. J. Kern, D. H. Werner, A. Monorchio, L. Lanuzza and M. J. Wilhelm, “The design synthesis of multiband artificial magnetic conductors using high impedance frequency selective surfaces,” in IEEE Transactions on Antennas and Propagation, vol. 53, no. 1, pp. 8-17, Jan. 2005.

[13]M. Hosseini, A. Pirhadi, and M. Hakkak, “A novel AMC with little sensitivity to the angle of incidence using 2-layer Jerusalem Cross FSS,” in progress in Electromagnetics Research, Vol. 64, 43-51, 2006.

[14]R. G. Kouyoumjian and L. Peters, "Range requirements in radar cross-section measurements," in Proceedings of the IEEE, vol. 53, no. 8, pp. 920-928, Aug. 1965.

[15]M. Le Goff, N. Adnet, N. Gross, L. Duchesne, A. Gandois and L. Durand, “A novel and innovative near field system for testing radomes of commercial aircrafts,” 2017 Antenna Measurement Techniques Association Symposium (AMTA), Atlanta, GA, 2017, pp. 1-5.

[16] C. Hu, N. Li, W. Chen and S. Guo, “A Near-Field to Far-Field RCS measurement method for multiple-scattering target,” IEEE Transactions on Instrumentation and Measurement, doi: 10.1109/TIM.2018.2882081.

[17] D. G. Falconer, "Extrapolation of near-field RCS measurements to the far zone," in IEEE Transactions on Antennas and Propagation, vol. 36, no. 6, pp. 822-829, June 1988.

[18]H. Ahmed, J. Hyun and J.R. Lee, “Development of scanning single port free space measurement setup for imaging reflection loss of microwave absorbing materials”, Measurement, vol. 125, 2018.

[19]N. Gagnon, J. Shaker, P. Berini, L. Roy and A. Petosa, “Material characterization using a quasi-optical measurement system,” in IEEE Transactions on Instrumentation and Measurement, vol. 52, no. 2, pp. 333-336, April 2003.

[20]E. Hajisaeid, A. F. Dericioglu and A. Akyurtlu, “All 3-D Printed Free-Space Setup for Microwave Dielectric Characterization of Materials,” in IEEE Transactions on Instrumentation and Measurement, vol. 67, no. 8, pp. 1877-1886, Aug. 2018.

[21]Jun Gyu Yang, Nam Jin Kim, In Su Yeom, Hong Sik Keum, Young Joon Yoo, Young Ju Kim, Y.P. Lee, “Method of measuring the amounts of electromagnetic radiation absorbed and controlled by metamaterials in anechoic chamber,” in Measurement, vol. 95, pp. 328-338, Aug. 2017.

[22]M. D. Blech et al., "Time-Domain Spherical Near-Field Antenna Measurement System Employing a Switched Continuous-Wave Hardware Gating Technique," in IEEE Transactions on Instrumentation and Measurement, vol. 59, no. 2, pp. 387-395, Feb. 2010.

[23]M.E. De Cos and F. Las-Heras, “On the advantages of loop-based unit-cell’s metallization regarding the angular stability of artificial magnetic conductors,” Applied Physics A, vol. 118, no. 2, pp. 699-708, 2015.

[24]R. Panwar and J.R. Lee, “Performance and non-destructive evaluation methods of airborne radome and stealth structures,” Measurement Science and Technology, vol. 29, no. 6, 2018.

[25]T. M. Kollatou, A. I. Dimitriadis, S. D. Assimonis, N. V. Kantartzis, and C. S. Antonopoulos, “A family of ultra-thin, polarization-insensitive, multi-band, highly absorbing metamaterial structures,” Prog. Electromag. Res., vol. 136, 579-594, 2013.